

# Glide matching with binary and ternary zeotropic refrigerant mixtures

## Part 2. A computer simulation

P. A. Domanski, W. J. Mulroy and D. A. Didion  
Thermal Machinery Group, National Institute of Standards and Technology,  
Gaithersburg, MD 20899, USA  
*Received 26 July 1993*

The glide-matching study presented in Part 1 was a laboratory investigation which demonstrated the evaporator performance in detail. However, since it was not possible to instrument the condenser sufficiently, some computer simulation work was conducted using a semi-theoretical model CYCLE-11, which has been under continual development at NIST for the past five years. As in the experimental effort, R22, R142b, R22/142b, R23/22/142b and R23/142b working fluids were investigated, but the simulation work did not include heat pump operation with liquid-line/evaporator heat exchange. By utilizing the model to quantify entropy generation at various state points within the cycle, it was possible to locate the likelihood of temperature profile pinch points in both the condenser and evaporator. This information clarified the impact of non-linearities on the system performance. (Keywords: zeotropic mixtures; boiling points; refrigerant mixtures; simulation)

## Correspondances de glissement avec les mélanges frigorigènes zéotropes

### 2ème partie: Simulation sur ordinateur

*L'étude sur les correspondances de glissement présentée dans la première partie et effectuée en laboratoire décrivait en détail les performances d'un évaporateur. Cependant, étant donné qu'il n'était pas possible d'équiper le condenseur de façon suffisante, on a entrepris de simuler la même expérience sur ordinateur à l'aide d'un modèle semi-théorique CYCLE-11 que NIST développe depuis cinq ans. Comme pour l'expérience en laboratoire, on a étudié les fluides actifs R22, R142b, R22/142b, R23/22/142b et R23/142b mais pas l'exploitation d'une pompe à chaleur avec échange thermique entre conduites de liquide et évaporateur. L'utilisation de ce modèle pour quantifier l'entropie à différents points d'état du cycle a permis de mettre en évidence la vraisemblance des profils de température pour le condenseur et l'évaporateur. Ces données ont clarifié l'impact de la non-linéarité sur la performance du système.* (Mots clés: mélanges zéotropes; points d'ébullition; mélanges de frigorigènes; simulation)

#### Description of simulation model

The name CYCLE-11 is used by the authors to describe a family of semi-theoretical models used for evaluating the performance of different working fluids – including mixtures – in the vapour-compression cycle. The version of CYCLE-11 used in this study is described in reference 1. Only a short summary of the model is given here.

CYCLE-11 performs simulations at specified inlet and outlet temperatures of the heat transfer fluids (HTFs) at the evaporator and condenser. In the version of CYCLE-11 used in this study, these heat exchangers are represented by the effective average temperature differences between the refrigerant and heat transfer fluid,  $\Delta T_{hx}$ , which are input data. Specifying the same  $\Delta T_{hx}$  for different simulated cases asserts the same heat-exchanger heat flux for each simulation. This is because  $\Delta T_{hx} = Q/(UA)$ , where ( $U$ ) is the overall heat transfer coefficient and is assumed constant in the model. The criterion of equal heat flux for heat exchangers was postulated by McLinden and Radermacher<sup>2</sup> as the necessary condition for fair performance comparison of single-component refrigerants and mixtures. This criterion was observed

during the experimental work, to the degree it was possible in the laboratory environment, by adjusting compressor speed according to the capacity of the tested refrigerant or mixture. However, during simulation runs the constant  $Q/UA$  criterion was strictly implemented.

The model involves a polytropic compression process, condensation in a counter-flow heat exchanger, an isenthalpic expansion process, and evaporation in a counter-flow heat exchanger. Refrigerant pressure drop in the evaporator and condenser, refrigerant subcooling in the condenser, and refrigerant superheat in the evaporator are specified as input data. If performance of a zeotropic mixture is simulated, the model accounts for a non-linear temperature profile during a phase change by subdividing the heat exchangers into a maximum of 128 equal enthalpy subsections.

The model, CYCLE-11, was modified for this study to correspond better to the laboratory experiment. The representation of the compressor was upgraded by accounting for pressure drop at the cylinder suction and discharge valves. This pressure drop in the model is sensitive to refrigerant specific volume and refrigerant mass flow rate. The mass flow rate is affected by the

compressor speed which has to be provided to the model on a relative basis as a fraction of the compressor speed at a chosen reference simulation run. These representations, although simplistic, help to capture relative performance differences between studied refrigerants.

The output of CYCLE-11 was expanded to include entropy production information. This information is given in the form of entropy generation per unit mass of circulated refrigerant. Assuming an adiabatic compressor, entropy generated by the cycle is calculated by considering entropy generation in the heat sink and heat source:

$$\Delta S_{\text{cyc}} = \Delta S_{\text{sink}} + \Delta S_{\text{source}}$$

where

$$\Delta S_{\text{sink}} = \int \frac{dQ_{\text{sink}}}{T}$$

is entropy generation in the heat sink, and

$$\Delta S_{\text{source}} = \int \frac{dQ_{\text{source}}}{T}$$

is entropy generation in the heat source. Assuming constant specific heat of the heat-transfer fluid over the temperature range within the heat exchanger, the above integrals can be evaluated as  $mc_p \ln(T_{\text{out}}/T_{\text{in}})$  where  $m$  = mass flow rate,  $c_p$  = heat capacity,  $T_{\text{in}}$  = inlet temperature of HTF,  $T_{\text{out}}$  = outlet temperature of HTF of the heat transfer fluid in the heat sink or heat source.

Assuming no heat loss to the ambient, entropy generation in the evaporator and condenser is calculated by considering entropy change in the refrigerant and heat transfer fluid. For example, for the evaporator, the entropy production,  $\Delta S_e$ , is

$$\Delta S_e = \Delta S_{\text{source}} + \Delta S_r$$

where  $\Delta S_r = S_{\text{out}} - S_{\text{in}}$  is entropy change in refrigerant, calculated by refrigerant thermodynamic property relations, and  $\Delta S_{\text{source}} = mc_p \ln(T_{\text{out}}/T_{\text{in}})$  is entropy change in the heat-source HTF.

The refrigerant thermodynamic properties required in the cycle calculations are supplied as independent subroutines which are linked with the code for the cycle model. CYCLE-11 uses REFPROP routines<sup>3</sup>, which were developed based on the Carnahan–Starling–DeSantis (CSD) equation of state<sup>4</sup>.

CYCLE-11 does not involve transport properties, which implies that the transport properties of the studied fluids are the same. Using the REFPROP package, we screened liquid viscosity and liquid thermal conductivity – the two most influential transport properties<sup>5</sup> – to estimate the significance of neglecting these properties on performance prediction. We found liquid conductivity to be within 10% for all the working fluids tested (R22, R142b and their mixtures). Liquid viscosity of pure R22, R142b and R23 are significantly different from each other:  $\mu_{\text{R142b}}/\mu_{\text{R22}} \approx 1.74$  and  $\mu_{\text{R23}}/\mu_{\text{R22}} \approx 0.52$ . For the R22-based mixtures, liquid conductivities are within 25% of that of pure R22, and for R142b-based mixtures the differences are within 15%. Based on the sensitivity analysis of the impact of transport properties performed in reference 5 and considering the differences between the system employed in this investigation and that in the sensitivity study, our estimate is that the impact of neglecting transport properties in simulations should not

affect the coefficient of performance by more than 10% (conservative) or 5% (more realistic). The important difference between the system in the sensitivity study and the present work is a significantly larger evaporator and condenser used in this investigation, which resulted in a low heat flux and refrigerant mass flux making the transport properties less important.

### Computer simulations

The objective of the computer simulations was to obtain additional insight into the laboratory results. Simulation results are free of experimental scatter, which makes them particularly helpful in the investigation of small performance trends. Simulation results are also useful as a supplement to laboratory data in the areas where the experimental rig is not fully instrumented.

Because of the simplicity of CYCLE-11, a full agreement on an absolute basis was not expected between laboratory results and simulation results. The merit of CYCLE-11 is considered to be in relative performance evaluations. The simulations were performed at the same operating conditions as the tests with the exception of the refrigerant state at the condenser outlet where the computer model allows for strict control of this parameter. For mixtures involving R22 (ternary) simulations were performed at the compositions found during the tests. For the R23/142b mixture, simulations were performed at gradually changing mixture composition to cover the composition range of interest.

Simulations were performed at the following operating conditions:

- temperature of HTF entering/leaving the evaporator, 26.6°C/12.8°C (80°F/55°F);
- temperature of HTF entering/leaving the condenser, 27.8°C/47.2°C (82°F/117°F);
- average effective temperature difference for evaporator, 2.8°C (5°F);
- average effective temperature difference for the condenser, 2.8°C (5°F);
- saturated vapour leaving the evaporator;
- polytropic compression efficiency, 0.85;
- refrigerant temperature leaving the condenser within 0.6°C (1°F) of the HTF temperature entering the condenser. This was controlled by specifying appropriate refrigerant subcooling. The limiting case was a pinched condenser at the refrigerant exit with subcooling equal to zero;
- pressure drop in the evaporator 6.9 kPa (1 lbf in<sup>-2</sup>);
- pressure drop in the condenser 20.7 kPa (3 lbf in<sup>-2</sup>).

An example of a cycle simulated by CYCLE-11 is shown in Figure 1.

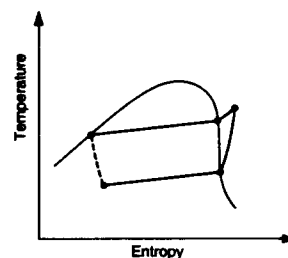


Figure 1 Cycle simulated by CYCLE-11

Figure 1 Cycle simulé par CYCLE-11

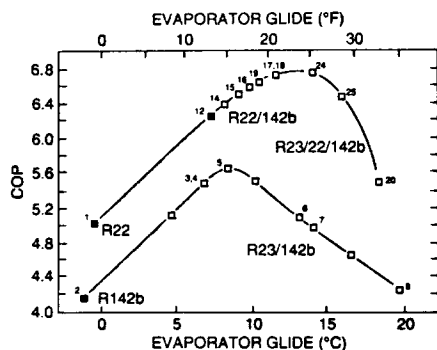


Figure 2 Adjusted COP simulation results (numbers 1–20 refer to Table 1 of Part 1)

Figure 2 Résultats ajustés de la simulation du COP (les numéros 1 à 20 font référence au tableau 1 de la partie 1)

An additional input to CYCLE-11 is the ratio of the compressor speed during a given run to the reference compressor speed. The reference compressor speed is the speed for a run used as a reference point. In this simulation study, the speed from a test of pure R142b was used as the reference because it represents the lowest volumetric capacity and thus the highest compressor speed.

Results from simulation runs are presented in graphical form. Figure 2 shows the coefficient of performance (COP) as a function of refrigerant glide in the evaporator. The values of COP shown in this figure are the simulated values adjusted by the ratio of the tested COP to the simulated COP for pure R142b (a factor equal to 0.79) to facilitate comparison with test data. CYCLE-11 overpredicted performance since, as a semi-theoretical cycle, it did not account for all losses. The lower curve represents the COP of the R23/142b mixture while the upper curve represents the COP of the R22-based mixtures. The numbers on both curves represent simulated performance at the mixture composition of the test identified by this number in Part 1 of this paper. The exception are numbers 24 and 25, which represent mixtures not tested in the rig: R23/22/142b (6/51/43) for point 24 and R23/22/142b (8/49.5/42.5) for point 25. These additional points demonstrated uniformity in the performance prediction by filling in gaps on the COP curve of the ternary experimental data.

Comparing the adjusted simulation results shown in Figure 2 and experimental results shown in Figure 7 of Part 1, it may be noted that the adjusted COP values consistently agree with the laboratory results. Also, CYCLE-11 predicted correctly the peaks of COP for both mixtures at approximately 8.3°C (15°F) and 12.8°C (23°F) evaporator glide. This agreement establishes confidence in the simulation results presented in the following figures.

Entropy generation in a process or a cycle is a measure of its irreversibility. Some interesting insight is given by Figures 3 and 4, which present entropy generation for the R23/142b mixture and the R23/22/142b mixture, respectively. The presented entropy generation corresponds to the same cooling duty for each simulated case (the cooling duty provided by 0.45 kg (1 lb) of pure R142b was used as the reference).

Four lines are presented in each entropy generation figure. The bottom line represents entropy generation in

the evaporator. The second line represents entropy generation in the condenser, while the third line shows the sum of the entropy generations for both heat exchangers. The top line shows total entropy production by the cycle. The difference between this top line and the line below is descriptive of irreversibilities in the compressor and the expansion device. Using the evaporator temperature glide as an index, the points of the minimum entropy production by the cycle correspond to the maximum COP values shown in Figure 2.

Two additional facts are worth further comment. First, for both mixtures (i.e. R23/142b and R23/22/142b) the cycle minimum entropy production occurs at the point of the minimum entropy production in the heat exchangers. This point coincides with minimum entropy generation in the condenser just before it pinches; that is, at the point of minimum temperature difference between the refrigerant and heat transfer fluids. Second, comparison of total entropy generation for the heat exchangers and the cycle in Figures 3 and 4 shows the better performance of the ternary refrigerant due to glide matching and the fact that it is a better refrigerant for the studied cycle. If Figures 3 and 4 were superimposed, it could be seen that the lines representing total entropy production for both heat exchangers (third line from the bottom on each figure) would almost coincide for the evaporator glide range from 0°C (0°F) to 8.3°C (15°F). This indicates that irreversibilities in this operating range for both heat exchangers in both cycles are the same. Therefore, the better COP of the mixture involving R22

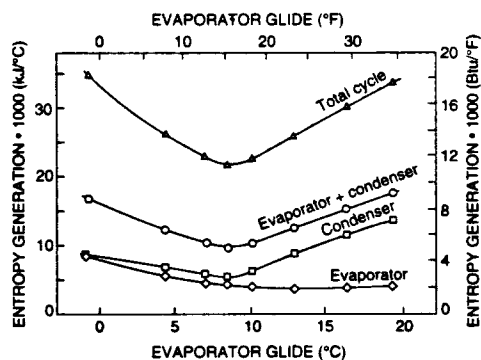


Figure 3 Total entropy generation for R23/142b binary mixture

Figure 3 Entropie totale pour le mélange binaire R23/142b

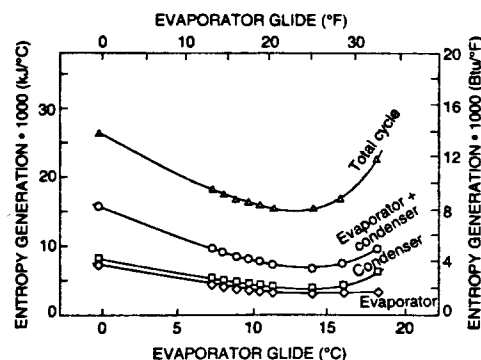


Figure 4 Total entropy generation for R23/22/142b ternary mixture

Figure 4 Entropie totale pour le mélange ternaire R23/R22/R142b

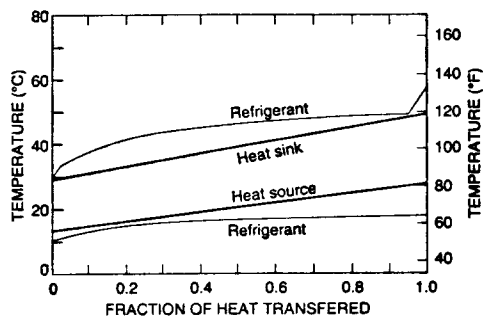


Figure 5 Heat exchangers temperature profiles for R23/142b (4/96 wt%)

Figure 5 Profils des températures des échangeurs thermiques pour R23/142b (4/96% wt)

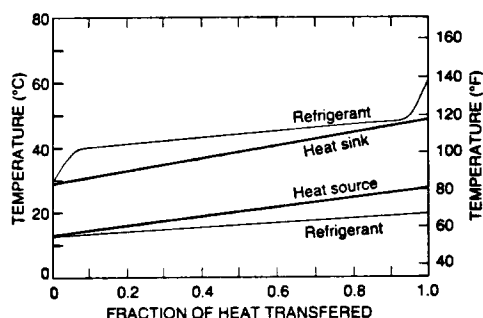


Figure 6 Heat exchangers temperature profiles for R22/142b (48/42 wt%)

Figure 6 Profils des températures des échangeurs thermiques pour R22/142b (58/42% wt)

(i.e. the ternary) is due to lower irreversibilities in the compression and expansion processes.

Figures 5–8 present refrigerant and HTF temperature profiles. The temperatures are presented as a function of the fraction of heat transferred in the evaporator and the condenser. Figures 5 and 6 present temperature profiles for R23/142b and R22/142b, respectively, for the evaporator glide at which heat exchanger irreversibilities for both mixtures are about the same.

The composition and operating conditions simulated in Figure 5 are the same as test number 5 in Table 1 of Part 1 of this paper. It was the maximum COP achieved for any composition of this binary mixture. Therefore, these temperature profiles probably represent the best compromise for minimizing the combined irreversibilities in the condenser and evaporator.

Figure 6 is a different binary mixture and simulates the conditions and composition of test number 12 in Table 1 of Part 1. Note also that the simulated evaporator temperature profile is quite similar to the measured one shown in test number 12 in Figure 6 of Part 1; as was Figure 5 compared to test number 6 of Figure 6 of Part 1. Since both of these simulations had a similar temperature glide and heat exchangers performance, the differences in COP (noted in Figure 5 of Part 1) are attributed to the differences in refrigerant properties and are not due to any zeotropic effect.

For the zeotropic effect (i.e. glide matching) the simulations of Figures 7 and 8 should be compared. Here we can see that the addition of the intermediate component (in this case R22) results not only in the

linearization of the evaporator refrigerant temperature profile but also a considerable reduction of the condenser temperature profiles difference through linearization. This latter point could not be determined by experiment since the condenser was not sufficiently instrumented. Note that the resulting COPs of the simulation in Figure 8 are shown in Figure 2 of this paper as point 24, which is a simulation result. Figure 7 temperature profiles are a simulation result for a case quite similar to the measured data of test number 7 in Table 1, Part 1.

As noted earlier, the addition of R23 to a mixture for these operating conditions may or may not be helpful to the system performance. By comparing the binary cases represented in Figure 5 (which is test number 5 in Figure 2 of this paper and Table 1 of Part 1) with Figure 7 (which is test number 7 in Figure 2 of this paper and Table 1 of Part 1) one can see that the addition of R23 reduces the system COP. On the other hand, the ternary cases Figure 6 (which is test number 12 in Figure 2 of this paper and Table 1 of Part 1) compared with Figure 8 (which is simulation result number 24 of Figure 2) shows an increase in system COP. This is because the zeotropic effect (i.e. the reduction of average temperature differences between the refrigerant and the HTFs) overcomes the negative effects of a lower critical point mixture caused by the increase in R23 proportion.

### Concluding remarks

Cycle simulation is quite useful when used in conjunction with a laboratory test program. It reduces scatter in the results allowing for a clearer picture of trends. It allows

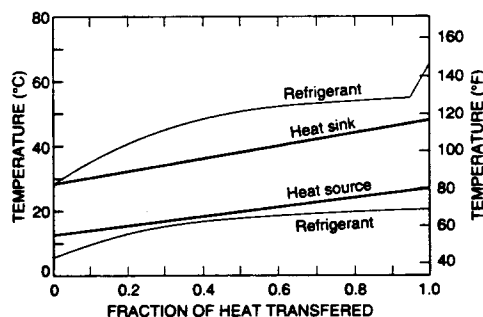


Figure 7 Heat exchangers temperature profiles for R23/142b (9/91 wt%)

Figure 7 Profils des températures des échangeurs thermiques pour R23/142b (9/91% wt)

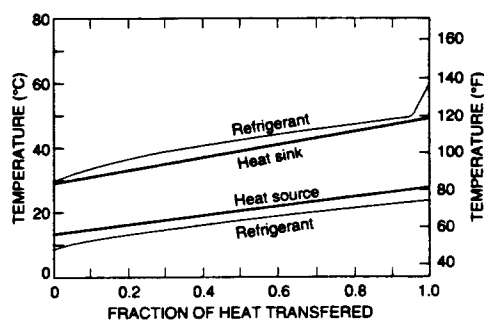


Figure 8 Heat exchangers temperature profiles for R23/22/142b (6/51/43 wt%)

Figure 8 Profils des températures des échangeurs thermiques pour R23/22/142b (6/51/43% wt)

for insight into components that were not thoroughly instrumented and for filling in intermediate data points or extending the operation range not practical for an experiment. For this study's purpose, the simulation included an entropy generation analysis for the major components and showed that the condenser benefited most by the conversion of a binary to a ternary: a conclusion that could only be speculated on if the study had been limited to the laboratory.

Ternary zeotropes offer an additional degree of freedom over binaries, at the price of increased complexity. For the purposes of this study, three components were selected based solely on their widely varying normal boiling points, to ensure significant non-linearity in one of the binary's temperature-enthalpy profiles. The interjection of a third component with an intermediate normal boiling point can reduce this non-linearity and allow the heat exchanger irreversibilities to be reduced because the average temperature difference between the fluids is reduced. For this study, the interjection of R22 between R23 and R142b caused this to happen. A second case where the third component may be useful is the addition of a low boiling point (high pressure) component to a binary zeotrope in order to increase the volumetric capacity and zeotropic tempera-

ture glide. For our selection of R23 added to the R22/142b binary, the additional temperature glide was achieved and the linearity of the temperature profile allowed for utilization of more heat exchanger area, less temperature differences between heat exchange fluids and thus an improved utilization of the Lorenz concept.

#### References

- 1 Domanski, P., McLinden, M. A simplified cycle simulation model for performance rating of refrigerants and refrigerant mixtures *Int J Refrig* (1992) **15** 81-88
- 2 McLinden, M., Radermacher, R. Methods for comparing the performance of pure and mixed refrigerants in the vapour compression cycle *Int J Refrig* (1985) **10** 318-325
- 3 Gallagher, J., McLinden, M., Morrison, G., Huber, M., Ely, J. Thermodynamic properties of refrigerants and refrigerant mixtures database (REFPROP, Version 3.0) *NIST Standard Data Base 23* National Institute of Standards and Technology, Gaithersburg, MD (1992)
- 4 DeSantis, R., Gironi, F., Marrelli, L. Vapor-liquid equilibrium from a hard-sphere equation of state *Ind Eng Chem Fundam* (1976) **15** 183-189
- 5 Domanski, P., Didion, D. Impact of refrigerant uncertainties on prediction of vapor compression cycle performance *NBSIR 86-3373* National Institute of Standards and Technology, Gaithersburg, MD (December 1986)